A New Phase of Hydroquinone and Its Thermodynamic Properties

Motosuke Naoki,* Takashi Yoshizawa, Nobuaki Fukushima, Motonari Ogiso, and Masaki Yoshino

Physical Chemistry Section, Bioscience Department, Faculty of Engineering, Gunma University, Kiryu, Gunma 376-8515, Japan

Received: February 9, 1999; In Final Form: May 21, 1999

Hydroquinone crystals have been found to undergo first-order phase transition to a denser polymorph with an enthalpy increment, as does resorcinol. The phase stable at room temperature (called α) transforms to the new phase (designated δ) only under elevated pressures. $P-V-T$ relations of the new phase have been measured, and characteristics of the transitions and the triple point among the α phase, the δ phase, and the liquid have been estimated from the thermodynamic consistency. The thermal expansion coefficient, the internal pressure, and the heat capacities of the δ phase are significantly larger than those of the α phase. Rigid-body vibrations and/or librations may play an important role in the αδ transition. Contributions of hydrogen bonds and the structure of the δ phase are discussed.

1. Introduction

Hydroquinone (1,4-benzenediol) has been extensively studied by X-ray diffraction from 1877[1−3] and is known to form three crystalline modifications, called as α, β, and γ,[4,5] near room temperature under atmospheric pressure. The α structure is capable of clathrating certain small molecules,[6,7] and its density is 1.364 g cm^{-3}.[7] The β form can clathrate many small molecules when crystallized in their presence.[8−13] The free β form without filling the cavities by guest molecules has a very loose packing[14−17] and its density is 1.258 g cm^{-3}.[17] The γ form obtained by sublimation[1,5,18] or by rapid evaporation[19] has a dense packing and its density is 1.380 g cm^{-3}.[19]

The α form is stable at room temperature, and the β and γ forms both change spontaneously into the α form. Taking into account the existence of the dense γ form of which structure was considered from the point of view of packing by Kitaigorodskii,[18] we may expect to find an equilibrium higher-density modification of hydroquinone, as with the β phase of resorcinol (1,3-benzenediol),[20] under some moderate pressures.

A first-order like transformation by compression from the low-density amorphous ice to the high-density amorphous ice was discovered by Mishima et al.,[21−23] and similar transformations have been found in SiO_2, GeO_2, BeF_2, and GaSb glasses.[24,25] These transformations, which have been observed in tetrahedral network glasses, are accompanied with a decrease in volume and an increase in entropy, as with the αβ transition of resorcinol. The glassy state, however, is essentially nonequilibrium, which makes it difficult to understand the glass−glass transformations. A detailed analysis on the equilibrium transition from low-density to high-density polymorph with positive latent entropy for crystals with three-dimensional hydrogen-bond network may give a clue to understand the glass−glass transition.

2. Experimental Section

Sample. Hydroquinone purchased from Nakarai Chemical Co. was purified by repeated zone-melting. The sample contained in a glass tube was sealed in a vacuum and was moved through the zone-melting equipment (4 steps) at a rate of 12 h per run. After 15 runs (60 steps), the glass tube was broken and the sample was taken out. The density of the sample was measured by the floating method with use of carbon tetrachloride and *n*-hexane.

DTA. A sample of about 1 g was poured into one of chambers in a DTA cell made of stainless steel at 200 °C. The other chambers were filled with silicone oil (KF-96-30CS, Shin-Etsu Chemical Co.) to transmit the hydrostatic pressure. The difference in temperature between the sample and the transmitting medium was read by the alumel−chromel thermocouple, and the temperature was read by the another alumel−chromel thermocouple calibrated within ±0.02 K. The pressure was measured by a Heise bourdon gauge with an automatic compensator (Dresser Ind.) within ±0.1 MPa.

We have carried out the DTA measurements under 0.1∼100 MPa about 90 times to outline the phase diagram in the following way. After the crystallization of the sample was confirmed, the temperature was raised to 380 K and the pressure was elevated near a desired pressure. Since the impulse of the regulation of pressure concealed small peaks, we closed the valve of the pump and raised the temperature up to the peak temperature of the melting at a heating rate of about 0.8 K min^{-1} without any regulation of pressure. Therefore, the present DTA experiments were not strictly isobaric and the pressure increased by about 1∼10 MPa (it depended on the seal of every pressure valve) during one heating scan. Just after passing through the melting point, the temperature was lowered and the pressure was released. In the present DTA measurements, the sample was not sealed from the transmitting medium (silicone oil) and the small DTA peak became smaller after several runs. We used about 30 different samples in the present experiments.

***P−V−T* Relations.** The pressure pycnometer made of Pyrex glass was designed for measuring the latent volume and the $P-V-T$ relations. It has six nodes with Pt wires, and the height of the mercury column can be detected from the outside of the pressure vessel. The apparent $P-T$ isochores obtained by the pycnometer are at the apparent constant volume of the pyc-

* Author to whom correspondence should be addressed.

10.1021/jp990480k CCC: $18.00
Published on Web 07/14/1999

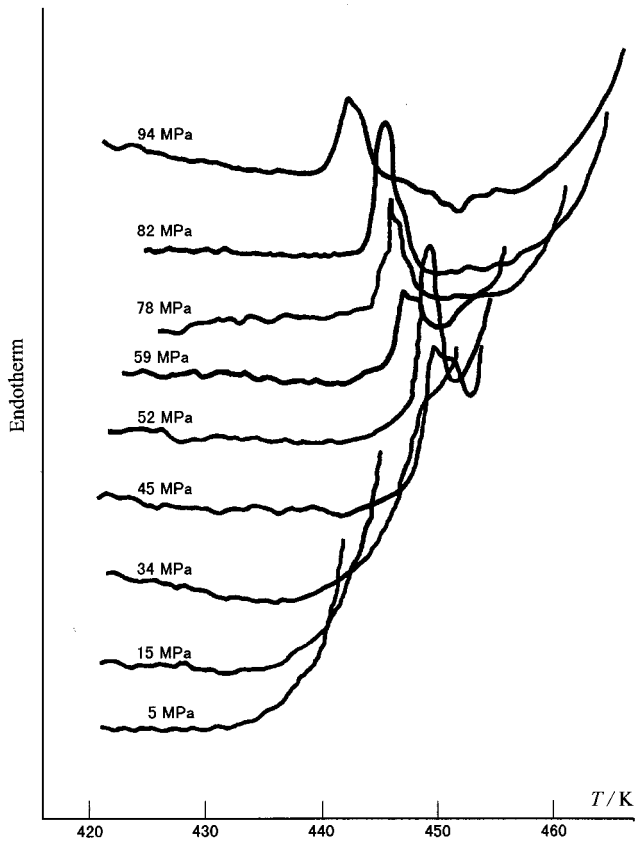

Figure 1. Examples of the small DTA peaks. The pressures around the small peaks are indicated.

nometer, and the volume of the sample can be obtained from the volumes of the pycnometer and mercury at each temperature and pressure. Details of the pycnometer, the procedure of measurements, and calculations of the sample volume are in the earlier paper.[20]

3. Results

DTA. We observed two endotherm DTA peaks above 40 MPa, a small one at a lower temperature and a large one pertaining to the melting. Figure 1 shows several examples of the small endotherm peaks. The small peak shifts to lower temperatures as the pressure increases. The small peaks were clearly distinguishable from the melting peaks above 40 MPa, but only shoulders or only small tops of peaks on the melting envelopes were observed between 30 and 40 MPa, and any signs of small peaks could not be detected below 25 MPa. We designate here the phase between the small peak and the melting peak as the δ phase.

Temperatures of the DTA peaks in the heating scans are plotted in Figure 2. The slope of the $\alpha \rightarrow \delta$ transformation temperature, $dT_{\alpha\rightarrow\delta}/dP$, is -0.0945 ± 0.0056 K MPa^{-1} from the linear fitting to the small peaks (closed symbols in Figure 2) above 40 MPa. The slope of the melting of δ, dT^{δ}_{m}/dP, is 0.2324 ± 0.0047 K MPa^{-1} from the melting peaks (open symbols in Figure 2) above 40 MPa. The slope of the melting of α, dT^{α}_{m}/dP, below 20 MPa, unfortunately, cannot be determined because of its narrow range, which will be discussed in the following section. The atmospheric melting temperature of α determined by the dilatometory is 446.7 ± 0.3 K,[26] which agrees with the DTA melting peaks within ± 1.4 K.

Hysteresis of the $\alpha \rightarrow \delta$ and $\delta \rightarrow \alpha$ Transformations. Figure 3 shows an example of the hysteresis of the $\alpha \rightarrow \delta$ and $\delta \rightarrow \alpha$ transformations in the apparent $P-T$ relations obtained by the pressure pycnometer. After we had measured the $P-T$ relation of α (open circles), we raised the temperature from 432.1 K under about 90 MPa as shown by the arrow. Then we observed that the mercury touched again the same Pt−mercury contact at 453.5 K under 86.8 MPa (open circles). This means that the dilation of the sample and mercury due to the 21.4 K increase was almost compensated by the volume decrease (the latent volume) accompanied with the $\alpha \rightarrow \delta$ transformation. After measuring the $P-T$ relation of δ, we carried out the tracing survey of the same Pt−mercury contact (closed circles) by lowering the temperature as shown by the arrow. It deviated from the $P-T$ line of δ at about 440.9 K (lower by about 7 K than the DTA $\alpha \rightarrow \delta$ transformation temperature). It finally merged in the $P-T$ line of α at 421.8 K under 45.8 MPa and reproduced the $P-T$ line of α as shown by closed circles. Such hysteresis was observed at every Pt−mercury contact, and the $P-T$ line in each phase was reversibly reproducible. This may strongly support that the $\alpha\delta$ transition is a first-order phase transition.

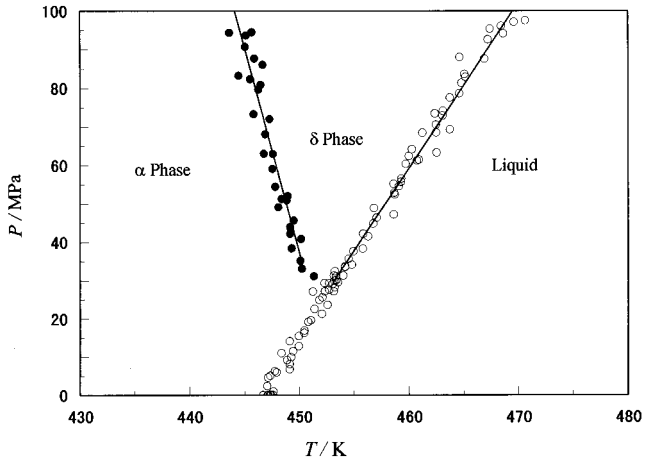

Figure 2. Temperatures of the DTA peaks. Closed symbols are for the $\alpha \rightarrow \delta$ transformation and open symbols are for the melting of α or δ. Lines are linear fittings of the $\alpha \rightarrow \delta$ transformation and the melting of δ above 40 MPa.

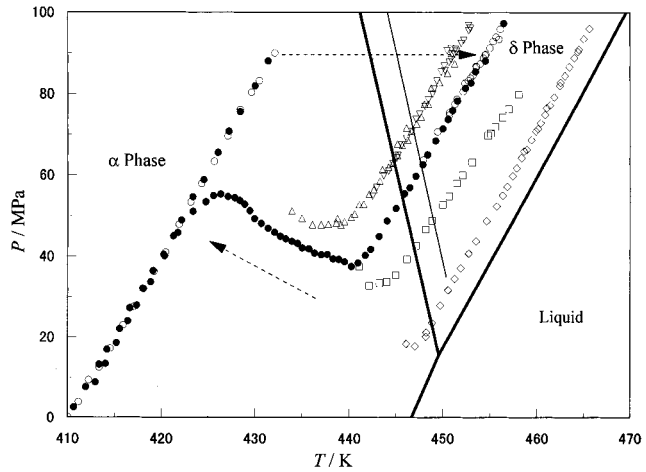

Figure 3. $T-P$ relations by the pressure pycnometers and an example of the hysteresis of the $\alpha \rightarrow \delta$ and $\delta \rightarrow \alpha$ transformations. The same symbols indicate the same Pt−mercury contact of the pycnometer. Dotted line is $T_{\alpha\delta}$ from DTA, and solid lines are the estimated equilibrium transitions.

***P−V−T* Relations of the δ Phase.** We obtained five $P-T$ lines for δ. Each volume of the sample was calculated by subtracting the volume of mercury from the volume of the

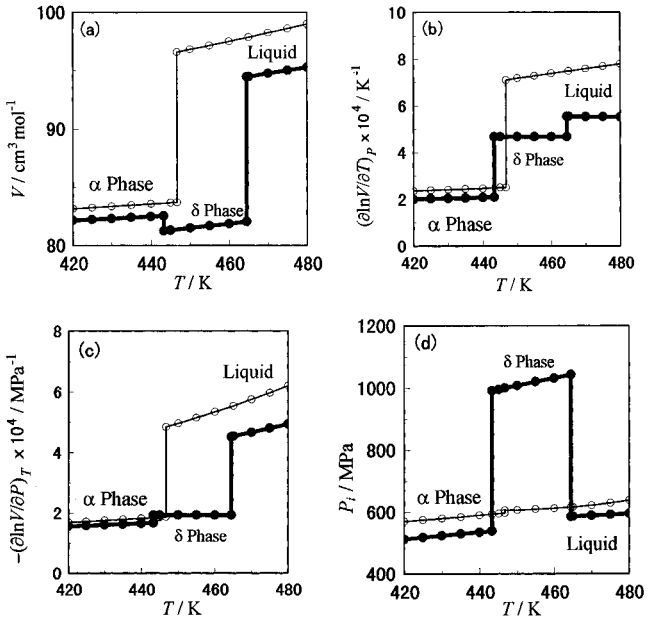

Figure 4. (a) The molar volume, (b) the thermal expansion coefficient, (c) the isothermal compressibility, and (d) the internal pressure. Open circles are for α and the liquid under atmospheric pressure. Closed circles are for α, δ, and the liquid under 78.5 MPa.

TABLE 1: *P-V-T* Relations of the δ Phase

V at 452.0 K and 70 MPa, cm^3 g^{-1}	0.74220 ± 0.00025
$(\partial \ln V/\partial T)_P \times 10^4$, K^{-1}	4.685 ± 0.095
$-(\partial \ln V/\partial P)_T \times 10^4$, MPa^{-1}	1.939 ± 0.065

pycnometer, based on the density from the floating method, 1.35603 ± 0.00037 g cm^{-3}, of α at 301.4 K under atmospheric pressure. Considering the phase diagram supposed from the DTA peaks in Figure 2, the range of δ is very limited. Therefore, we represent the $P-V-T$ relations of δ by the average thermal expansion coefficient, $(\partial \ln V/\partial T)_P$, under the higher pressures, by the average isothermal compressibility, $-(\partial \ln V/\partial P)_T$, around 452 K, and by the reference volume at 452.0 K under 70 MPa, which are listed in Table 1. The $P-V-T$ relations are summarized in Figure 4 in comparison with those of α and the liquid.[26] The isothermal compressibility of δ is almost the same as α, whereas the thermal expansion coefficient of δ is much larger than that of α and rather close to that of the liquid. As a result, it gives rise to the considerably large internal pressure defined by

$$P_i \equiv (\partial E/\partial V)_T = T\gamma - P = -T(\partial \ln V/\partial T)_P/(\partial \ln V/\partial P)_T - P \quad (3.1)$$

where E is the internal energy and γ is the thermal−pressure coefficient defined by $(\partial P/\partial T)_V$. P_i is the slope of the average intermolecular potential and the large P_i corresponds to the steep slope of the potential energy as a function of volume. This suggests that the short-ranged van der Waals (vdW) energy rather than the hydrogen-bond (HB) energy plays an important role in δ.

4. Estimation of the Phase Diagram

Since the hysteresis is observed, superheating and supercooling are unavoidable in the αδ transition. The α→δ transformation temperatures obtained from the heating scans of the DTA should be somewhat higher than the equilibrium ones. We will try to estimate the phase diagram from the thermodynamic consistency.

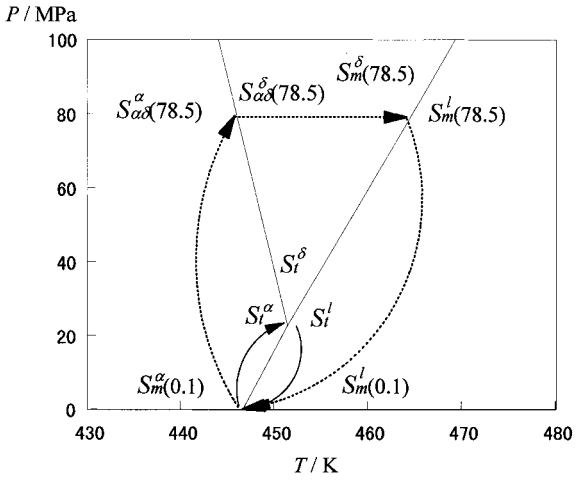

Figure 5. The entropy cycles to estimate the phase diagram.

We assume that the slope of $T_{\alpha\to\delta}$ against P from DTA is almost equal to the slope of the equilibrium transition temperature, $T_{\alpha\delta}$, i.e., $dT_{\alpha\delta}/dP \approx dT_{\alpha\to\delta}/dP$. If the equilibrium $T_{\alpha\delta} - P$ relation and triple point were found, any cyclic calculation of the thermodynamic state quantity should close from the thermodynamic consistency. We have adopted the following two cyclic processes of the entropy as shown schematically in Figure 5: (i) $S^{\alpha}_m(0.1)$ (the entropy of α at T^{α}_m under 0.1 MPa) → $S^{\alpha}_{\alpha\delta}(78.5)$ (at $T_{\alpha\delta}$ under 78.5 MPa) → $S^{\delta}_{\alpha\delta}(78.5)$ (the entropy of δ at $T_{\alpha\delta}$ under 78.5 MPa) → $S^{\delta}_m(78.5)$ (at T^{δ}_m under 78.5 MPa) → $S^{l}_m(78.5)$ (the entropy of the liquid at T^{δ}_m under 78.5 MPa) → $S^{l}_m(0.1)$ (at T^{α}_m under 0.1 MPa) → $S^{\alpha}_m(0.1)$; and (ii) $S^{\alpha}_m(0.1) \to S^{\alpha}_t$ (at the triple point) → $S^{\delta}_t \to S^{l}_t \to S^{l}_m(0.1) \to S^{\alpha}_m(0.1)$.

The entropy difference within each phase, e.g., $S^{\alpha}_{\alpha\delta}(78.5) - S^{\alpha}_m(0.1)$, can be calculated from the volume dependence of the thermal−pressure coefficient by use of the usual thermodynamic relation:

$$\Delta S = \int_{V_1}^{V_2} \gamma \, dV \quad (4.1)$$

The latent entropy at each transition point, e.g., $\Delta S_{\alpha\delta} = S^{\delta}_{\alpha\delta}(78.5) - S^{\alpha}_{\alpha\delta}(78.5)$, can be obtained from the latent volume by use of the Clapeyron equation:

$$(dT/dP)_{\text{transition}} = \Delta V_{\text{latent}}/\Delta S_{\text{latent}} \quad (4.2)$$

At the triple point, we can use the following relation.

$$\Delta S^{\alpha}_m = \Delta S_{\alpha\delta} + \Delta S^{\delta}_m \quad (4.3)$$

When one cyclic calculation is performed, we will obtain $\Delta S^{\alpha}_m = S^{l}_m(0.1) - S^{\alpha}_m(0.1)$ and dT^{α}_m/dP from eq 4.2. Drawing the T^{α}_m line from T^{α}_m (0.1 MPa) with the slope dT^{α}_m/dP, we will obtain a new triple point as the intersection of the $T^{\alpha}_m - P$ and $T^{\delta}_m - P$ lines. Repeating the cyclic calculations and minimizing the deviation between the two cyclic processes, we have estimated the characteristics of the transitions, which are listed in Table 2. The transition lines are shown in Figure 3. The triple point among α, δ, and the liquid is lower by 1.8 K in temperature and by 6.8 MPa in pressure than the crossover point of $T_{\alpha\to\delta}$ and T^{δ}_m from DTA.

The estimated value of ΔH^{α}_m at 0.1 MPa is 30.8 ± 1.2 kJ mol^{-1}, which is larger than the value 27.11 ± 0.42 kJ mol^{-1} obtained from calorimetry by Andrews et al.[27] The assumption, $dT_{\alpha\delta}/dP \cong dT_{\alpha\to\delta}/dP$, means that the superheating depends little

TABLE 2: Characteristics of the Transitions at the Triple Point, at 0.1 MPa, and at 78.5 MPa

transition	αδ transition	melting of α	melting of δ
		Triple Point	
T_t, K		449.6 ± 0.5	
P_t, MPa		15.7 ± 2.4	
ΔH, kJ mol^{-1}	4.7 ± 0.3	30.3 ± 0.8	25.8 ± 0.5
ΔS, J mol^{-1} K^{-1}	10.4 ± 0.7	67.3 ± 1.7	57.4 ± 1.2
ΔV, cm^3 mol^{-1}	−1.04 ± 0.03	12.54 ± 0.14	13.6 ± 0.2
$(dT/dP)_{transition}$, K MPa^{-1}	−0.1003 ± 0.0067	0.1863 ± 0.0047	0.2368 ± 0.0047
P, MPa	78.5	0.1	78.5
T, K	443.3	446.7 ± 0.3	464.5
ΔH, kJ mol^{-1}	5.7 ± 0.7	30.8 ± 1.2	24.3 ± 0.9
ΔS, J mol^{-1} K^{-1}	12.9 ± 1.5	69.1 ± 2.6	52.4 ± 2.0
ΔV, cm^3 mol^{-1}	−1.30 ± 0.05	12.88 ± 0.13	12.41 ± 0.18

on pressure. The δ→α transformation temperature from the pressure pycnometer in Figure 3 seems to give somewhat larger $dT_{\delta\to\alpha}/dP$ than $dT_{\alpha\to\delta}/dP$. Supercooling rather than superheating, however, is usually more influenced by environments, and the cause of this difference is not obvious at present.

5. Thermal Properties of δ

δ exists only under elevated pressures, and it is usually difficult to carry out calorimetric experiments. When the $P-V-T$ relations are available for α, δ, and the liquid, however, the thermal properties of δ can be calculated from those of α and the liquid under 0.1 MPa. The isobaric heat capacity, C_P, of α and the liquid under 0.1 MPa was measured by Andrews[28] and Andrews et al.[27] Integrating C_P and C_P/T from the reference point, $(T_0, P_0) = (420\ \text{K}, 0.1\ \text{MPa})$ to T^{α}_m, the enthalpy, H, and S of the liquid at 0.1 MPa can be obtained by use of the latent quantities. From the familiar thermodynamic relations, the differences in C_P, H, and S between P_0 and P (chosen as 78.5 MPa) at each temperature are given by

$$C_P(P)-C_P(P_0) = -T\int_{P_0}^{P}(\partial^2 V/\partial T^2)_P\,dP \qquad (5.1)$$

$$H(P)-H(P_0) = -T\int_{P_0}^{P}(\partial V/\partial T)_P\,dP + \int_{P_0}^{P} V\,dP \qquad (5.2)$$

$$S(P)-S(P_0) = -\int_{P_0}^{P}(\partial V/\partial T)_P\,dP \qquad (5.3)$$

H of δ at $T_{\alpha\delta}$ and T^{δ}_m can be obtained with $\Delta H_{\alpha\delta}$ from α and with ΔH^{δ}_m from the liquid, respectively. Assuming C_P of δ to be constant in the region between $T_{\alpha\delta}$ and T^{δ}_m under 78.5 MPa, we have C_P of δ from

$$C_P = [H(T^{\delta}_m) - H(T_{\alpha\delta})]/(T^{\delta}_m - T_{\alpha\delta}) \qquad (5.4)$$

and we have S, H, and C_V of δ in that region. The results are summarized in Figure 6, in which the melting of α under 0.1 MPa, the αδ transition, and the melting of δ under 78.5 MPa are shown.

Both S and H of δ are somewhat larger than those of α, but significantly smaller than those of the liquid. C_P and C_V of δ, however, are considerably larger than those of α and almost the same as those of the liquid. Although values of C_P and C_V of δ are sensitive to the errors in the latent enthalpies, this tendency remains within the overall error limits. As the intermolecular interactions have only small effect on C_V, C_V is considered as a measure of the kinetic contribution. The event of the larger C_V of δ rather than that of α suggests that some kinetic rigid-body motions such as vibrations and librations are more active in δ than in α.

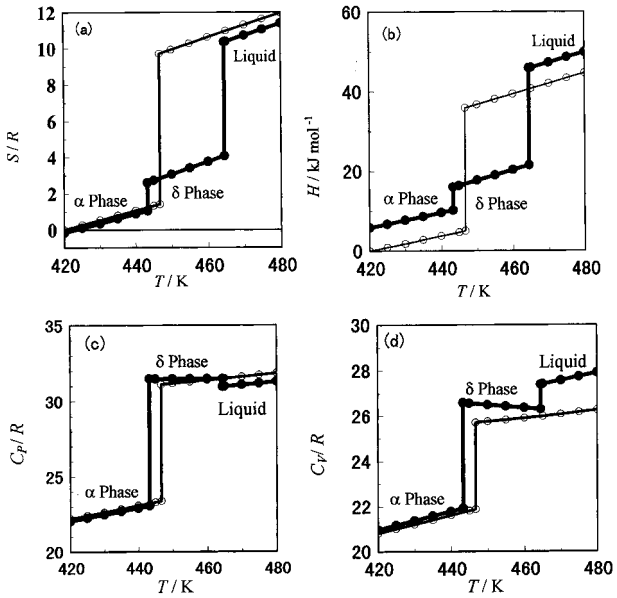

Figure 6. (a) The entropy, (b) the enthalpy, (c) the heat capacity at constant pressure, and (d) the heat capacity at constant volume. The reference point for S and H is 420 K under atmospheric pressure. Open circles are for α and the liquid under atmospheric pressure. Closed circles are for α, δ, and the liquid under 78.5 MPa.

6. Structure

We will discuss the structure of δ on the basis of the information obtained above. The first problem is whether δ would be identical with the β or γ modification studied by the X-ray diffraction. As the β form has a very loose packing with the low density of 1.258 g cm^{-3}, it is out of the question. The γ form, of which structure was considered from the point of view of packing by Kitaigorodskii,[18] has a higher density of 1.380 g cm^{-3} at room temperature.[19] The density of δ at $T_{\alpha\delta}$ (443.3 K, 78.5 MPa) is 1.355 g cm^{-3} and its extrapolation to room temperature and atmospheric pressure gives 1.37∼1.40 g cm^{-3}, which is almost the same as that of the γ form. The γ form investigated by Maartmann-Moe belongs to the monoclinic system of $P2_1/c$, $a = 8.07$, $b = 5.20$, $c = 13.20$ Å, $\beta = 107°$ with four molecules in the unit cell.[19] Hydrogen-bonded molecular sheets parallel to the bc plane are piled up along the a axis, and there are no hydrogen bonds but vdW forces keeping the sheets together along the a axis.[18,19] This structure seems to match the high P_i of δ. As the angles of O−H···O of the γ form are slightly smaller than those of the α form, the HB energy of the γ form would be somewhat weaker than that of the α form. This decrease in the HB energy contributes to the increase in the latent enthalpy, but may not be enough to compensate for the increase in the vdW energy and to produce the positive latent heat. The source of the high C_V of δ, which suggests the rigid-body vibrations and/or librations, is not clear from the crystallographic data of the γ form.[18,19] It should be noted that we could supercool δ to room-temperature neither in the DTA cell nor in the pressure pycnometer.

A simple potential model, which is composed of the Lennard-Jones (LJ) potential and the HB potential, has been proposed to analyze the HB contribution in the αβ transition of resorcinol.[20] As the model has been made for crystals with the three-dimensional HB network, the γ form is beyond the scope of this model. In this model, the configurational energy of the j phase is expressed by

$$E_c^j = E^*[(1 - \xi^j g^j x)(y^4 - 2y^2) + \xi^j e^j x(y^4 - 1.125y)] \quad (6.1)$$

where

$$y = V^*/V,\ E^* = (1/2)Nz\epsilon_{LJ},\ e^j = \epsilon_{HB}^j/\epsilon_{LJ},\ x = N_{HB}/Nz \quad (6.2)$$

ξ^j is the extent of the intermolecular hydrogen bonds in each phase defined by $0 \le \xi^j \le 1$. y is the reduced density; V^*, the vdW volume of the molecule; ϵ_{LJ}, the energy constant of the LJ potential; ϵ_{HB}^j, the energy constant of the HB potential of the j phase; N, the Avogadro number; N_{HB}, the number of groups forming hydrogen bonds; z, the coordination number per molecule; and g^j, the geometrical parameter which corrects an excluded volume effect of each hydrogen bond in the j phase. The internal pressure is expressed by

$$P_i^j = -(E^*/V^*)[4(1 - \xi^j g^j x)(y^5 - y^3) + \xi^j e^j x(4y^5 - 1.125y)] \quad (6.3)$$

We have adopted the vdW volume of hydroquinone as $V^* = 61.92$ cm^3 mol^{-1} obtained by Bondi's method,[29] the fraction of the HB contacts as $x = 4/z$, the extent of hydrogen bonds in α as $\xi^\alpha = 1$, and have assumed that ϵ_{LJ} of α is the same as that of δ. Values of the parameters, ϵ_{LJ}, ϵ_{HB}^α, ϵ_{HB}^δ, ξ^δ, g^α, g^δ, and z, can be obtained by adjusting the theoretical P_i^α, P_i^δ, and $E_c^\delta - E_c^\alpha$ to the experimental ones. In the αδ transition, however, the kinetic contribution to the internal energy of δ cannot be ignored, and some ambiguity may remain in the results.

Results for $\xi^\delta = 1$ (four hydrogen bonds per molecule as with α), $\xi^\delta = 0.75$ (three hydrogen bonds per molecule), $\xi^\delta = 0.5$ (two hydrogen bonds per molecule), and $\xi^\delta = 0.25$ (one hydrogen bond per molecule) are listed in Table 3. A measure of the stability of hydrogen bonds in δ is given by the difference between the value of E_{vdW}, the vdW energy per one coordination, and the value of E_{HB}, the HB energy per one hydrogen bond. That is, if $E_{HB}^\delta < E_{vdW}^\delta$, some of the hydrogen bonds are not necessary and may be broken to reduce the free energy. This is the case for $\xi^\delta = 1$ and $\xi^\delta = 0.75$. From this analysis, we can only say that, if δ has a three-dimensional HB network, the number of hydrogen bonds per molecule are two or fewer.

7. Conclusion

The α phase of hydroquinone has been found to transform to a denser polymorph, δ, with positive latent enthalpy under elevated pressures. The $P-V-T$ relations of δ show a high thermal expansion coefficient and an abnormally high internal pressure. This suggests that the vdW energy rather than the HB energy may be predominant in δ. The heat capacity of δ is much higher than that of α and close to that of the liquid. The high heat capacity at constant volume of δ suggests that some rigid-body vibrations and/or librations may be present in δ.

While $\Delta V_{\alpha\delta}$ is negative, $\Delta S_{\alpha\delta}$ is positive at the αδ transition, as well as in the $\alpha\beta$ transition of resorcinol. Most of the positive latent entropy of the $\alpha\beta$ transition may be caused from the redistribution of protons in each hydrogen bond.[20] $\Delta S_{\alpha\delta}$, however, is much larger than $\Delta S_{\alpha\beta}$, the latent entropy of the $\alpha\beta$ transition, and another source of the entropy increase should be considered for the αδ transition. The difference in the heat capacity between α and β of resorcinol is very small,[27,28,30] whereas that between α and δ of hydroquinone is considerable. An entropy increase owing to kinetic motions in δ should be incorporated into $\Delta S_{\alpha\delta}$.

TABLE 3: Parameters in Eq 6.1 and the Energies per Coordination

ξ^δ	1	0.75	0.5	0.25
z	13	13.9	13.4	13.8
g^α	1.51	1.53	1.29	1.1
g^δ	1.02	1.26	1.33	1.35
E_{HB}^α, kJ mol^{-1}	−23.3	−22.3	−21.2	−16.9
E_{vdW}^α, kJ mol^{-1}	−14.7	−12.9	−13.3	−11.6
E_{HB}^δ, kJ mol^{-1}	−10.3	−12.0	−16.0	−15.9
E_{vdW}^δ, kJ mol^{-1}	−19.2	−15.5	−14.6	−12.0

The analysis with the simple potential model suggests that two hydrogen bonds per molecule at least are broken in δ, if δ has a three-dimensional HB network. This structure rather than the γ modification seems to be preferable to account for large kinetic contributions.

Since the entropy usually decreases as the volume decreases, the transitions with negative latent volume and positive latent entropy seems peculiar. The key to understanding such transitions is the source of the positive latent entropy. Now we have found two typical entropy sources in transitions accompanied with the breakdown of hydrogen-bond network by compression (or by increasing temperature). When C_V of the high-density phase is almost the same as that of the low-density phase as in resorcinol, the entropy source to stabilize the high-density phase may be the redistribution of protons in weakened hydrogen bonds. When C_V of the high-density phase is larger than that of the low-density phase as in hydroquinone, the entropy source may be the kinetic contribution. Considering a similarity in short-range structures between glass and crystal, this kind of entropy sources should play an important role on the stability of high-density glasses under compression.

References and Notes

(1) Lehmann, O. *Z. Kryst. Min.* **1877**, *1*, 43.
(2) Heydrich, K. *Z. Kryst. Min.* **1910**, *48*, 244.
(3) Becker, K.; Jancke, W. *Z. Phys. Chem.* **1921**, *99*, 242.
(4) Caspari, W. A. *J. Chem. Soc.* **1926**, 2944.
(5) Caspari, W. A. *J. Chem. Soc.* **1927**, 1093.
(6) Powell, H. M. *J. Chem. Soc.* **1948**, 61.
(7) Wallwork, S. C.; Powell, H. M. *J. C. S. Perkin II* **1980**, 641.
(8) Palin, D. E.; Powell, H. M. *Nature* **1945**, *156*, 334.
(9) Palin, D. E.; Powell, H. M. *J. Chem. Soc.* **1947**, 208.
(10) Palin, D. E.; Powell, H. M. *J. Chem. Soc.* **1948**, 815.
(11) Wallwork, S. C.; Powell, H. M. *J. Chem. Soc.* **1956**, 4855.
(12) Mak, T. C. W.; Tse, J. S.; Tse, C. S.; Lee, K. S.; Chong, Y. H. *J. C. S. Perkin II* **1976**, 1169.
(13) Boejens, C. A. J.; Pretorius, J. A. *Acta Crystallogr.* **1977**, *B33*, 2120.
(14) Kitaigorodskii, A. I. *Molecular Crystals and Molecules*; Academic Press: New York, 1973.
(15) Powell, H. M.; Riesz, P. *Nature* **1948**, *161*, 52.
(16) Evans, D. F.; Richards, R. E. *Nature* **1952**, *170*, 246.
(17) Lindeman, S. V.; Shklover, V. E.; Struchkov, Yu. T. *Cryst. Struct. Commun.* **1981**, *10*, 1173.
(18) Kitaigorodskii, A. I. *Dokl. Akad. Nauk SSSR* **1945**, *50*, 319.
(19) Maartmann-Moe, K. *Acta Crystallogr.* **1966**, *21*, 979.
(20) Yoshino, M.; Takahashi, K.; Okuda, Y.; Yoshizawa, T.; Fukushima, N.; Naoki, M. *J. Phys. Chem. A* **1999**, *103*, 2775.
(21) Mishima, O.; Calvert, L. D.; Whalley, E. *Nature* **1984**, *310*, 393.
(22) Mishima, O.; Calvert, L. D.; Whalley, E. *Nature* **1985**, *314*, 76.
(23) Mishima, O. *J. Chem. Phys.* **1994**, *100*, 5910.
(24) Sidorov, V. A.; Brazhkin, V. V.; Khvostantsev, L. G.; Lyapin, A. G.; Sapelkin, A. V.; Tsiok, O. B. *Phys. Rev. Lett.* **1994**, *73*, 3262.
(25) Brazhkin, V. V.; Lyapin, A. G.; Khvostantsev, L. G.; Sidorov, V. A.; Tsiok, O. B.; Bayliss, S. C.; Sapelkin, A. V.; Clark, S. M. *Phys. Rev. B* **1996**, *54*, 1808.
(26) Yoshino, M.; Yoshizawa, T.; Fukushima, N.; Mouri, A.; Naoki, M. To be published.
(27) Andrews, D. H.; Lynn, G.; Johnston, J. *J. Am. Chem. Soc.* **1926**, *48*, 1274.
(28) Andrews, D. H. *J. Am. Chem. Soc.* **1926**, *48*, 1287.
(29) Bondi, A. *Physical Properties of Molecular Crystals, Liquids, and Glasses;* Wiley: New York, 1968.
(30) Suga, H.; Nakatsuka, K.; Shinoda, T.; Seki, S. *Nihonkagakuzassi* **1961**, *82*, 29.